Pharm Res (2010) 27:2330–2342
DOI 10.1007/s11095-010-0120-z

RESEARCH PAPER

PEG-poly(amino acid) Block Copolymer Micelles for Tunable Drug Release

Andrei Ponta • Younsoo Bae

Received: 30 November 2009 / Accepted: 5 March 2010 / Published online: 6 April 2010

ABSTRACT

Purpose To achieve tunable pH-dependent drug release in tumor tissues.

Methods Poly(ethylene glycol)-poly(aspartic acid) [PEG-p(Asp)] containing 12 kDa PEG and pAsp (5, 15, and 35 repeating units) were prepared. Hydrazide linkers with spacers [glycine (Gly) and 4-aminobenzoate (Abz)] were introduced to PEG-p(Asp), followed by drug conjugation [doxorubicin (DOX)]. The block copolymer-drug conjugates were either reconstituted or dialyzed in aqueous solutions to prepare micelles. Drug release patterns were observed under sink conditions at pH 5.0 and 7.4, 37°C, for 48 h.

Results A collection of six block copolymers with different chain lengths and spacers was synthesized. Drug binding yields were 13–43.6%. The polymer-drug conjugates formed <50 nm polymer micelles irrespective of polymer compositions. Gly-introduced polymer micelles showed marginal change in particle size (40 ± 10 nm), while the size of Abz-micelles increased gradually from 10 to 40 nm as the polymer chain lengths increased. Drug release patterns of both Gly and Abz micelles were pH-dependent and tunable. The spacers appear to play a crucial role in controlling drug release and stability of polymer micelles in combination with block copolymer chain lengths.

Conclusion A drug delivery platform for tunable drug release was successfully developed with polymer micelles possessing spacer-modified hydrazone drug-binding linkers.

KEY WORDS controlled drug delivery · functional block copolymers · pH-sensitive drug release · polymer micelles · tunable drug release

A. Ponta • Y. Bae (✉)
Pharmaceutical Sciences, College of Pharmacy, University of Kentucky,
789 South Limestone,
Lexington, Kentucky 40536, USA
e-mail: younsoo.bae@uky.edu

INTRODUCTION

Chemotherapy has long been a prominent, reliable and common way of treating cancer (1). Mechanisms of drug action, including absorption, distribution, metabolism, and excretion (ADME) in the body are generally well-described prior to clinical applications. However, it is not unusual that chemotherapy is frequently restricted by serious toxic side-effects and drug resistance, which hinder the potential of most available drugs (2). The fact that cancer cells often show differential drug sensitivity, depending on disease stages and lesions, also makes chemotherapy challenging (3). Despite the urgent need, there are neither successful dosage forms nor therapeutic paradigms currently available to resolve these issues simultaneously for effective cancer chemotherapy. In an effort to overcome the limitations of current chemotherapy, this study develops a novel drug delivery system (DDS) that can achieve tunable pH-sensitive drug release in order to control spatial and temporal distribution of drugs specifically in tumor tissues.

The importance of spatial control of drug distribution can be observed in clinical experiences that show that toxic side-effects of chemotherapy are primarily due to non-specific accumulation of drugs in the body. Over the past decades, DDS using drug carriers, such as water-soluble polymers, liposomes and polymer micelles, have been developed by focusing on the reduction of drug toxicity through tumor-specific drug delivery (4). Previous results clearly demonstrate that chemotherapy with DDS leads to a significant decrease in systemic toxicity (5). The enhanced permeability and retention (EPR) effects explain the mechanism through which drug carriers can accumulate in tumor tissues for more prolonged time periods than small-molecule drugs, by taking advantage of leaky tumor blood vessels and immature lymphatic drainage (6–8). Prolonged accumulation of drug carriers in tumors eventually results in

a time-dependent increase in drug concentrations (9,10). This phenomenon is referred to as passive tumor targeting. Extensive preclinical and clinical studies show that DDS-based chemotherapy is highly promising in that tumor-specific delivery can suppress non-specific distribution of drugs in the body (11–13). Noticeably, these drug carriers can be functionalized further with tumor-targeting molecules, such as antibodies, ligands and aptamers, to more actively interact with cancer cells (14,15). This increases drug delivery efficiency in intracellular regions or any other targeted locations in the body. Distinguished from the passive tumor-targeting, this type of DDS is called active tumor-targeting.

To the contrary, little attention has been paid to temporal control of drug distribution in tumors to date. Studies frequently show that chemotherapeutic efficacy *in vivo* is dependent not only on drug concentrations but also therapeutic schedules (16–18). Nevertheless, a large number of DDSs have been developed primarily to improve solubility and tumor-specific accumulation of drugs. Considerable therapy may be achieved through targeted drug delivery while simultaneously reducing toxicity, yet therapeutic performance of drug carriers is often over- or underestimated by the extent of tumor-specific drug delivery efficiency. Therefore, it is hypothesized that the temporal control of drug distribution in tumor tissues would be as important as spatial control of tumor-specific drug accumulation. It would achieve effective chemotherapy that sensitizes cancer cells, which often develop drug resistance, in various disease stages. Recent studies support this hypothesis, demonstrating that cancer cells exposed to small amounts of drug over longer periods appear to be more sensitive to chemotherapy than the cells incubated with a higher drug dose for shorter exposure time (19). Even in identical cancer cell lines, a drastic change in drug response is seen during chemotherapy, requiring extensive and complicated design of regimens to modulate drug concentration levels, intervals, and retention time. These results support the rationale that the controlling of temporal distribution of anticancer drugs in tumor tissues would significantly improve therapeutic efficacy of conventional chemotherapy.

A reasonable approach for the development of tunable drug delivery systems may be to functionalize drug carriers whose physicochemical and pharmacokinetic properties are already characterized extensively in preclinical and clinical applications. For these reasons, tunable drug delivery systems are designed in this study by using poly(ethylene glycol)-poly(amino acid) block copolymer micelles as a DDS platform (20). Block copolymer micelles, or polymer micelles, are spherical nanoassemblies with <100 nm particle size (21,22). The polymer micelles are generally prepared from self-assembling block copolymers, which can be functionalized further with various molecules and functional groups for applications such as imaging, diagnosis, and treatment of tumors (23). The characteristic core-shell structures impart the micelles with unique capabilities of protecting hydrophobic and toxic drug payloads as well as functional groups from the outer environment (24). Animal studies show that the micelles avoid the body defense system *in vivo*, leading to prolonged plasma retention time and tumor-specific accumulation of toxic drugs (25–27). Facile chemical modifications can be readily made to the core domain without changing physicochemical properties of micelles (e.g. water-solubility, surface charge and particle size). Such unique properties and facile functionality distinguish the polymer micelles from other drug carriers (28).

Fig. 1 outlines the overall design of tunable pH-sensitive polymer micelles developed in this study. The polymer micelles are prepared from PEG-p(Asp) block copolymers as a scaffold. Carbazate linkers, comprised of hydrazide groups and spacers, are introduced to the scaffold (Fig. 1a). Degradable drug-binding hydrazone bonds are widely employed to achieve tunable pH-sensitive drug release for drugs possessing a ketone group (29). Similarly, it is expected that carbazate linkers can be used as pH-sensitive linkers. It must be noted that the hydrolysis rates of carbazate linkers are expected to be controlled more precisely by chemical modification of functional groups adjacent to the carbonyl of the carbazate group (30,31). Inserting a spacer affects the physiochemical properties of the scaffold, and a more detailed look into the effect of hydrophobicity as well as charge density on drug release patterns is being considered. Notably, the hydrolysis rate and drug release rate could be tuned by changing the spacer. It is known that physiological pH is 7.4, while intratumoral pH is lowered to 6.8–7.2. On the other hand, intracellular pH is more acidic, reaching 5.0 in endosomes and lysosomes (32). Such differences in pH throughout the body would permit these micelles to control the conditions of drug release in various locations differentially (33,34). DOX, a widely used anticancer drug, is used in this study as a model drug because it has a ketone group at its C13 position and also possesses the spectrometric advantages over detection of color and fluorescence. Also significant is the fact that the linkage between carbazate and DOX permits the release of the drug itself, not an analogue, while maintaining the structure of the block copolymer scaffold (35). Therefore, polymer micelles reported in this study will possibly deliver anticancer drugs to tumor tissues selectively (Fig. 1b) and achieve tunable release according to regimens designed (Fig. 1c).

A collection of six block copolymers with different compositions is synthesized and characterized to prepare polymer micelles. Drug release studies are analyzed extensively in order to investigate the relationship between block copolymer structures, hydrolysis rates of linkers, drug loading,

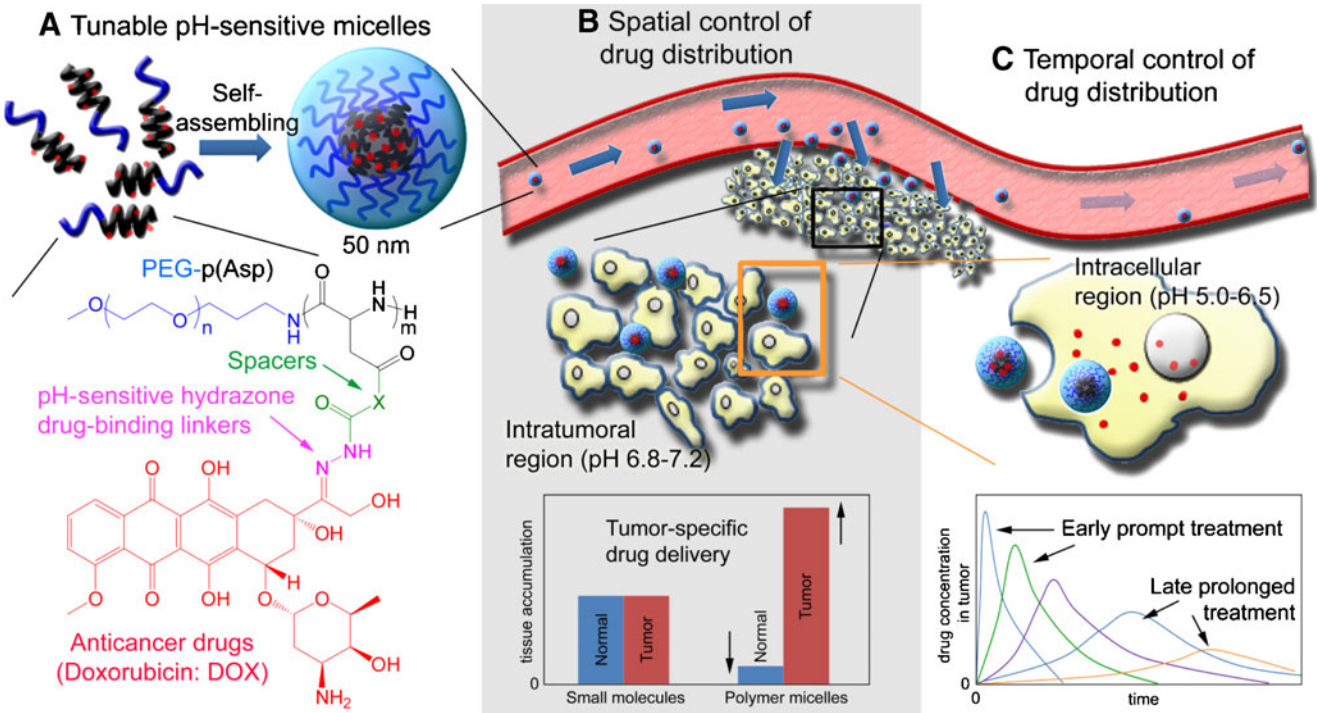

Fig. 1 Spatial and temporal control of drug distribution using tunable pH-sensitive polymer micelles.

drug release, and micelle stability. These factors are critical in the design of optimal regimens that modulate drug concentration levels, intervals and retention time for future preclinical applications.

MATERIALS AND METHODS

Materials

L-aspartic acid β-benzyl ester, anhydrous hydrazine, benzene, N,N'-diisopropylcarbodiimide (DIC), 4-(dimethylamino)pyridine (DMAP), N-Hydroxysuccinimide (NHS), blue dextran, N,N-dimethylformamide, anhydrous N,N-dimethylformamide (DMF), anhydrous dimethylsulfoxide (DMSO), dimethylsulfoxide-d6 (DMSO-*d6*), doxorubicin hydrochloride (DOX), ethanolamine, anhydrous ethyl ether, anhydrous hexane, anhydrous tetrahydrofuran (THF), triphosgene, acetate buffer solution, phosphate buffer solution, methyl 4-aminobenzoate, O-Benzotriazole-N,N,N',N'-tetramethyl-uronium-hexafluoro-phosphate (HBTU), sodium hydroxide (NaOH) were purchased from Sigma-Aldrich (USA). Glycine-OMe is from Novabiochem (SUI). α-Methoxy-ω-amino poly(ethylene glycol) (PEG-NH_2, MW = 12,266) was purchased from NOF Corporation (Japan). Regenerated cellulose dialysis bags with molecular weight cut off (MWCO 6–8,000), Slide-A-Lyzer® dialysis cassettes with 10,000 MWCO and Sephadex LH-20 gels were purchased from Fisher Scientific (USA). Amicon-Ultra centrifugal ultrafiltration devices with MWCO 30,000 were purchased from Millipore (USA).

Monomer Synthesis

β-Benzyl-L-aspartate N-carboxy anhydride (BLA-NCA) was prepared using the Fuchs-Farthing method. Briefly, triphosgene (2.88 g, 9.7 mmol) was added to β-benzyl -L-aspartate (5.0 g, 22.4 mmol) in dry THF (100 mL). The reaction was allowed to proceed under N_2 at 45°C until the solution became clear. Anhydrous hexane was then slowly added to the solutions until NCA crystals showed and disappeared quickly. The solution was stored in −20°C for recrystallization of BLA-NCA. Purified BLA-NCA with a needle-like shape was used for block copolymer synthesis.

PEG-PBLA Block Copolymer Scaffold Synthesis

Ring-opening polymerization of BLA-NCA was initiated from the terminal primary amine group of PEG-NH_2 as reported previously (36). Briefly, PEG was freeze-dried prior to the reaction and used as a macroinitiator. Three compositions of block copolymers containing 5, 15 and 35 β-benzyl-L-aspartate (BLA) were synthesized by increasing the amount of BLA-NCA with respect to PEG. In regard to the number of repeating units, weighed BLA-NCA (0.46 μmol, 183 μmol, 361 μmol) monomers and PEG (42 μmol, 183 μmol, 183 μmol) were dissolved in separate flasks containing anhydrous DMSO at 50 mg/mL under N_2

atmosphere. Dissolved monomers were added to the PEG solution in order to produce block copolymers with a narrow range. The polymerization was then carried out at 45°C for 2 days. PEG-PBLA block copolymers were obtained after precipitation of the reaction solution in anhydrous ethyl ether. Solubility test confirmed that unreacted BLA readily dissolves in ether, while PEG-PBLA precipitates. White powders were collected, and impurities in the supernatant were discarded. Repeating ether precipitations multiple times ensures the purity of PEG-PBLA. Ether precipitation also removes DMSO, and freeze drying allows for a pure final product. In the subsequent step of the synthesis process, dialysis is performed, which will also remove any remaining BLA. No PEG-NH_2 should be present after the initial reaction, since NCA was added in excess and the reaction was allowed to proceed for 2 days. The successful removal of unreacted monomers was confirmed, and this was supported by the ratios between monomer added and number of repeating units obtained.

Linker Design and Drug Conjugation

Carbazate drug-binding linkers were introduced to PEG-p(Asp) scaffolds by the modification of the side chains according to the following steps: spacer coupling and end-group functionalization with hydrazine (Fig. 2). Side chains of PEG-PBLA block copolymers were deprotected with 0.1 N NaOH, providing PEG-p(Asp) block copolymers. PEG-p(Asp) (12 μmol) was freeze-dried and subsequently modified with spacers, such as glycine methyl esters (Gly) (129 μmol, 400 μmol, 700 μmol) and methyl 4-aminobenzoate (Abz) (130 μmol, 450 μmol, 680 μmol) using HBTU in DMF at 40°C overnight. The amount of spacers added was increased in respect to the number of Asp repeating units (5, 15 and 35). At the end of the reaction, precipitates were removed through filtration. Side-chain modified block copolymers were first precipitated in ether and then dialyzed in a deionized water methanol (50:50) solution to remove unreacted Gly and Abz. The methyl esters of the spacers were replaced with hydrazide (Hyd) through aminolysis reaction. Excess hydrazine with respect to number of repeating units (145 μmol, 490 μmol, 890 μmol and 134 μmol, 515 μmol, 856 μmol for the Gly and Abz modified block copolymers, respectively) was reacted with PEG-p(Asp-Gly) (5.9 μmol, 6.5 μmol, 5.1 μmol) and PEG-p(Asp-Abz) (5.4 μmol, 6.8 μmol, 4.9 μmol) in DMF at 40°C for 1 h to obtain PEG-p(Asp-Gly-Hyd) and PEG-p(Asp-Abz-Hyd) block copolymers, respectively. Impurities were removed through repetitive ether precipitation. Final products were collected by freeze-drying.

Prepared block copolymers were conjugated with the chemotherapeutic agent DOX in DMSO at 30°C for 2 days. Because it contains a ketone group at the 13 position, DOX reacts with the carbazate linkers on the block copolymer through a hydrazone bond. DMSO and unreacted drugs were removed by ether precipitation. DOX-conjugated

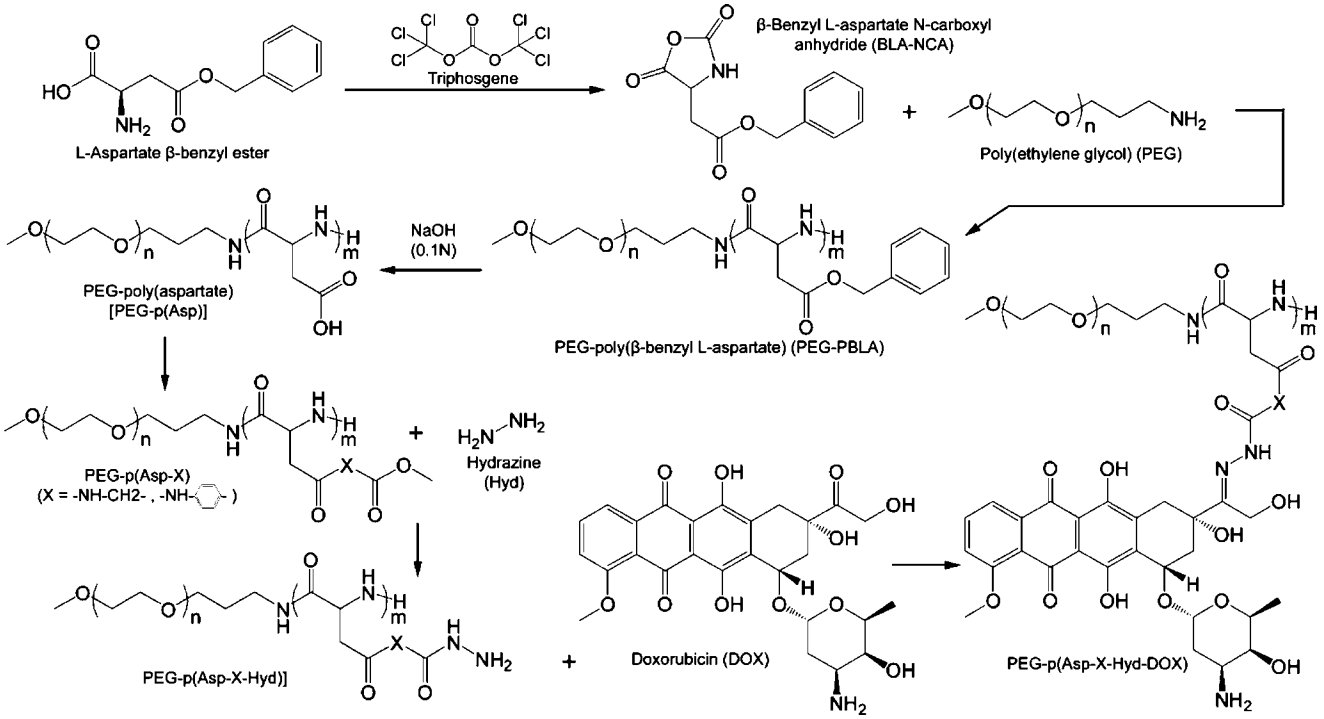

Fig. 2 Synthesis protocol.

block copolymers were purified further by a Sephadex LH20 column in methanol, removing remaining impurities smaller in size than final block copolymers, including drug molecules physically bound to the polymer. For block polymers with longer chain lengths (35 repeating units), minimal amounts of DMSO were added to completely dissolve them in methanol. Polymer fraction from the column was collected in a round-bottom flask, followed by rotatory evaporation to remove methanol. Benzene was added to the round-bottom flask to dissolve a thin film of block copolymers with short chain lengths (12–5 and 12–15). The solutions were sonicated and freeze-dried. Twelve to 35 block copolymers with poor solubility in benzene were redissolved in DMSO, precipitated in ether and collected by freeze-drying from benzene/methanol mixed solvents. Degree of DOX conjugation for these block copolymers was determined using UV-Vis colorimetric analysis at 480 nm.

Polymer Micelle Preparation

Preparation of micelles was achieved in two different ways according to solubility of block copolymers in aqueous solutions. The block copolymers with 5 and 15 BLA repeating units were dissolved in deionized water and sonicated to prepare micelles. Block copolymers containing 35 repeating units were found to be insoluble in deionized water directly through reconstitution; thus, micelles were formed using a dilution method. The drug-conjugated block copolymers were first dissolved in DMSO (<5 mg/mL) and then titrated into a 10-fold deionized water solution. Organic solvents were completely removed by repeating centrifugal ultrafiltration [molecular weight-cut off (MWCO) 30,000 g/mol] with aqueous solutions to obtain clear concentrated polymeric micelle solutions. The drug loading content of the micelles was determined by UV-Vis colorimetric analysis at 480 nm for DOX. Micelle solutions with different block copolymer compositions were diluted into the same drug concentration, and the sample aliquots were stored at 4°C until use.

Analytical Methods

^{1}H-NMR measurements were performed in DMSO-*d6* at 300 MHz normal proton frequencies. The device was equipped with FTS systems preconditioning a spectrometer composed of internal temperature controller and inclusion transfer line. Sample temperature was set at 25°C for all measurements.

Polymer micelle size was characterized by dynamic light scattering (DLS). A Zetasizer Nano-ZS (Malvern, UK) equipped with He-Ne laser (4 mW, 633 nm) light source and 173° angle scattered light collection configuration was used to determine polymer micelle mean diameters. The hydrodynamic diameter of micelles was calculated based on the Stokes-Einstein equation. Correlation function was curve-fitted by a cumulant method to calculate mean size. For each block copolymer composition, three separate micelle solutions were prepared to provide repetitions for precise analysis. Number distributions of particle sizes are presented as the average diameter with standard deviation.

Drug loading and conjugation were determined using a SpectraMax M5 (Molecular Devices, USA) equipped with variable spectrum filters and SoftMax Pro software. DOX was used as a standard because of its strong light absorption at 480 nm. This fingerprint peak was determined by taking the spectra of DOX from 400 nm to 800 nm. Subsequent spectra were taken of PEG-p(Asp-Gly-Hyd) and PEG-p(Asp-Abz-Hyd) block copolymers, which confirmed that the absorbance profile of DOX does not change after chemical modification. The calibration curve for DOX was prepared with standard samples ranging from 250 μM to 0.98 μM. Using this standard curve, drug loading and drug release were measured. Characteristic absorbance of DOX was measured in aqueous solutions using a 96-well plate at 25°C for drug concentration quantification.

Drug Release Study

Micelle solutions were put in two Slide-A-Lyzer® (Thermo Scientific, USA) 0.5 mL dialysis cassettes with a MWCO of 10,000 g/mol in preparation for release experiments. Two cassettes were used for each experiment in order to take measurements at multiple intervals. For each composition, 0.5 mL of micelle solution was placed into each dialysis cassette, totaling 1.0 mL. The cassettes were placed in 4.0 L of 10 mM buffer solutions with different pHs. Acetate and phosphate buffer solutions were used for pH 5.0 and 7.4, respectively. Temperature was held constant at 37°C throughout the experiments, mimicking physiological conditions in the body. The sampling time intervals were 0, 0.5, 1, 3, 6, 24 and 48 hrs. The first cassette was used for sampling at 0.5, 1 and 3 hrs, with the remainder of the samples taken out of the second cassette. At each time interval, a sample of at least 50 μL was withdrawn and collected in microtubes for spectroscopic analysis. Three repetitions of each release experiment were conducted.

Statistics

Statistical analysis was performed using Tukey's Multiple Comparison Test or t-test at 5 % significance level. Data were recorded as mean ± standard deviation. All experiments were done at least in triplicate as specified in the results section. Data analyses were performed using Microsoft Excel (2007).

RESULTS

Denotation

Block copolymer chain compositions are denoted as X-Y, where X and Y stand for PEG MW$\times 10^{-3}$ and number of PBLA repeating units, respectively. Drugs as well as functional groups conjugated to the side chains are described sequentially in the parentheses of p(Asp). For instance, PEG-p(Asp) block copolymers with carbazate drug-binding linkers are denoted as PEG-p(Asp-X-Hyd), where X indicates spacers (Gly or Abz). The micelles from PEG-p(Asp-Gly-Hyd-DOX) and PEG-p(Asp-Abz-Hyd-DOX) block copolymers are described as Gly micelles and Abz micelles, respectively.

Monomers and Block Copolymer Scaffolds Synthesis

Monomers of β-Benzyl L-aspartate N-carboxy anhydride (BLA-NCA) were synthesized successfully, based on the protocol reported previously (37). Final monomer products were purified through repeated washing with anhydrous hexane, resulting in needle-like BLA-NCA crystals. Poly (ethylene glycol)-poly(β-benzyl L-aspartate) (PEG-PBLA) block copolymers with various chain lengths were synthesized by changing the amount of BLA-NCA monomers. The number of repeating units of PBLA was precisely controlled by proportionally adding BLA-NCA monomers. ^{1}H-NMR was used to quantify the actual number of BLA repeating units on each block copolymer. PEG with a known molecular weight of 12,000 kDa has a prominent peak at 3.5 ppm (Fig. 3a, denoted by letter a). BLA contains a benzyl group with a peak observed at 7.3 ppm (Fig. 3a, denoted by letter b). Using the ratio of the area of the PEG peak to the area of the BLA peak, the number of BLA repeating units was determined. Integral ratios of the three block copolymers synthesized, in the form of PEG:BLA, were 1091:25, 1091:77 and 1091:172. It was determined that compositions of prepared PEG-PBLA were 12–5, 12–15 and 12–35. These were close to the target compositions of 12–10, 12–20 and 12–40. Benzyl esters of PEG-PBLA were removed completely by dissolving block copolymers in 0.1 NaOH. Hydrolysis reaction in NaOH yielded a clear polymer solution upon the completion of the deprotection. Final products provided PEG-p(Asp) block copolymers, which were used as a scaffold to introduce drug-binding linkers.

Linker Design and Drug Conjugation

Gly and Abz were coupled to the carboxyl groups of PEG-p(Asp) to introduce spacers to hydrazide linkers (Fig. 3). Coupling reactions using DIC, NHS and DMAP

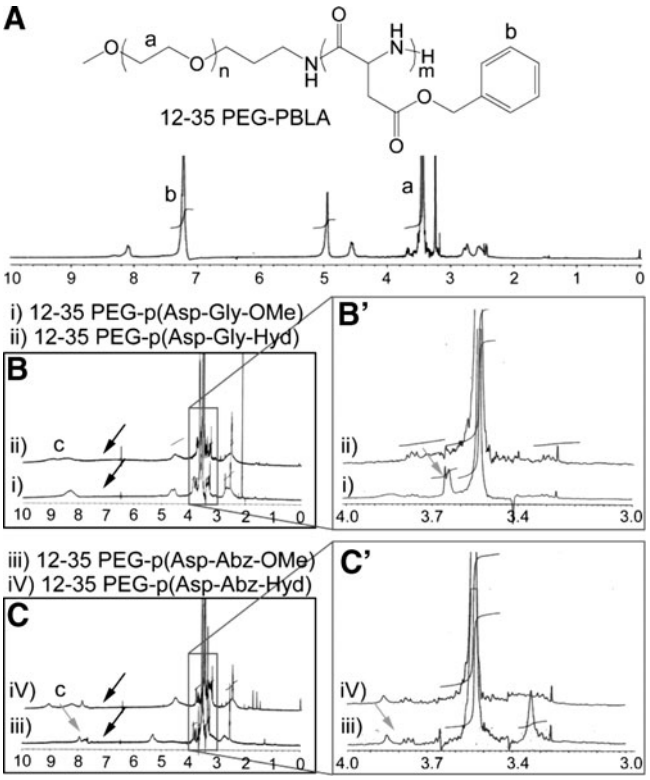

Fig. 3 ^{1}H-NMR spectra.

were initially performed for Gly and Abz, yet proved to be unsuccessful. Different coupling reagents were tested until settling with HBTU, which yielded the most promising results. Solubility test confirmed that all of the reactants completely dissolved in the water/methanol mixed solvent and were therefore removed after dialysis. ^{1}H-NMR confirmed the conjugation of Gly and Abz to PEG-p(Asp) (Fig. 3). The benzyl peak which originally resulted from PBLA (Fig. 3a) disappeared for both Abz and Gly conjugation, confirming deprotection of PEG-PBLA (black arrows in Fig. 3b and c). To clearly see the methyl ester peaks, a portion of the ^{1}H-NMR spectra from 3 to 4 ppm was magnified. Methyl ester peaks of Gly-OMe appeared at 3.65 ppm as a result of the spacer conjugation (a gray arrow in Fig. 3b'). However, the methyl peak of Abz-OMe, expected to show at 3.8 ppm (a gray arrow in Fig. 3c'), was less prominent, even though the benzyl peaks of Abz-OMe were shown at 7.8 ppm (a gray arrow in Fig. 3c). Functionalizing the end-group of the block copolymer was accomplished by replacing the methyl esters with Hyd. The replacement of methyl esters with hydrazide was also confirmed by ^{1}H-NMR, which shows that methyl peaks disappeared and broad peaks of hydrazide at around 9 ppm newly appeared (Fig. 3b and c, denoted by letter c). The PEG-p(Asp-Gly) spectra contained a clear methyl ester peak at 3.65 ppm, which subsequently disappeared once reacted with hydrazide (Fig. 3b'). Though the reactions

between hydrazide and the methyl esters of the side chains were confirmed, quantification of Gly, Abz and Hyd was unsuccessful due to peak overlapping and broadening. For these reasons, drug molecules bound to block copolymers were quantified and used for estimation of the minimal number of binding sites on each block copolymers.

DOX was conjugated to the PEG-p(Asp-Gly-Hyd) or PEG-p(Asp-Abz-Hyd) block copolymers through a hydrazone bond (Figs. 2 and 4) leading to the formation of PEG-p(Asp-Gly-Hyd-DOX) and PEG-p(Asp-Abz-Hyd-DOX). The reaction conditions for the DOX conjugation have been optimized through extensive testing of different solvents, temperatures and concentrations in previous studies. It has been determined that the drug binding reaction between DOX and hydrazide groups of the block copolymers do not require acid catalyst in DMSO. After ether precipitation and freeze drying, a Sephadex column in methanol was used to remove unreacted drug molecules. Two bands were observed in the column. A darker band passed through the column quicker, while a lighter band moved slower through the column. The darker band containing polymer-drug conjugates was collected successfully after column separation. Methanol was readily removed through rotary evaporation to form a thin film at the bottom of a round-bottom flask. Solubility of block copolymers differs in benzene, which hampered the collection of products by simple reconstitution and freeze-drying. Sonication of polymer-drug conjugates with short chain lengths (12–5, and 12–15) in benzene was effective to redissolve and freeze-dry the products. The conjugates with a longer chain length (12–35), however, were redissolved in DMSO for ether precipitation and freeze-dried from benzene/methanol mixed solvents.

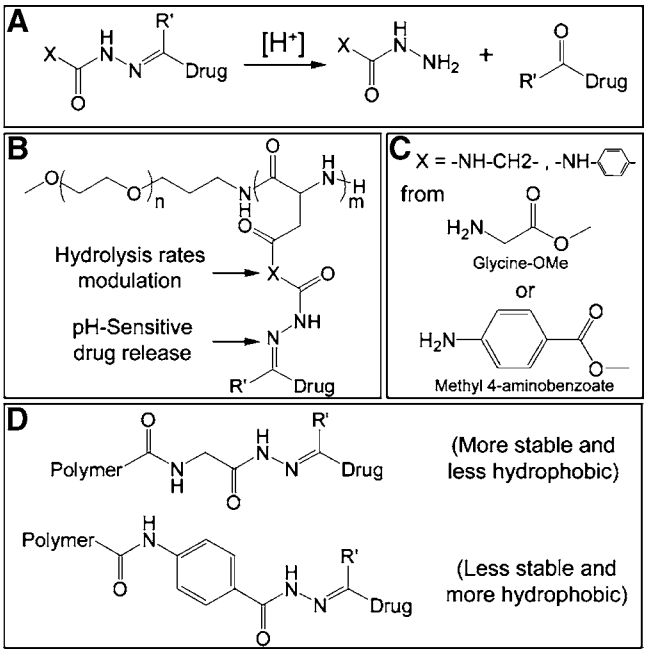

Fig. 4 Mechanisms of tunable pH-sensitive drug release control.

Drug loading of final products was determined using UV-VIS spectrometry at 480 nm (Table I). Drug loading was accounted for in three ways: 1) weight percent, 2) number of DOX molecules per block copolymer, and 3) percentage of DOX molecules bound in proportion to available linkers. Drug loading was successful in each of the six block copolymers, but the drug loading per binding site was not too ideal in some cases. Spacers introduced to the side chain of block copolymers used in this study seem to induce steric hindrance that might hamper further binding of DOX. Other factors, such as charge density, length of spacers, and lipophilicity of the micelle core, play a crucial role not only in drug binding but also drug release. Drug loading weight percent increased for both block copolymers from 2.8% to 32% and from 4.0% to 11% for PEG-p(Asp-Gly-Hyd-DOX) and PEG-p(Asp-Gly-Abz-DOX), respectively. It is apparent that increasing the chain lengths of PEG-p(Asp) scaffolds increases the number of DOX molecules bound to the block copolymer chain. The drug loading per binding site of PEG-p(Asp-Gly-Hyd-DOX) steadily increased with the increase of repeating units from 13% to 44%. For PEG-p(Asp-Abz-Hyd-DOX) with 5 and 15 repeating units, the drug loading per binding site was 20% and 22.5%, respectively. However, the drug loading per binding site decreased to 14% for the 12–35 composition, since only five DOX molecules bound to the block copolymer out of a possible 35 binding sites. Although increasing the number of repeating units in PEG-p(Asp-Abz-Hyd-DOX) increased the number of DOX molecules bound to the polymer chain, it seemed to show no influence on the drug loading per binding site.

Polymer Micelle Preparation

Polymer-drug conjugates were used to prepare polymer micelles as described in the experimental section. Characterization of micelles was conducted in aqueous conditions. It is intriguing that Gly and Abz micelles with compositions of 12–5 and 12–15 readily formed uniform micelles by simply dissolving the block copolymers in aqueous solutions. To the contrary, 12–35 did not dissolve in water readily and underwent precipitation. For this reason, polymer micelles from 12–35 were prepared by dissolving the polymer in DMSO first and titrating the solution in aqueous solutions. DMSO was completely removed from the solution by centrifugal ultrafiltration kits (MWCO 30,000 kDa). DLS measurements showed that each of the six compositions formed micelles with <50 nm particle size (Table II). Noticeably, Gly micelles maintained particle size between 40 and 45 nm, showing no significant difference

Table I Drug Entrapment Efficiency

Compound	Composition	Drug loading weight %	DOX molecule/block copolymer	Drug loading/binding site (%)
PEG-p(Asp-Gly-Hyd-DOX)	12–5	2.80	0.65	13
	12–15	10.4	3.03	20
	12–35	31.66	15.26	43.6
PEG-p(Asp-Abz-Hyd-DOX)	12–5	4.07	0.97	20
	12–15	10.92	3.38	22.5
	12–35	11.46	4.75	14

among the three different compositions. On the other hand, particle size of Abz micelles increased as the chain lengths increased. Particle sizes of micelles from 12–5, 12–15 and 12–35 were 11, 24 and 43 nm, respectively. The only composition that showed a similar particle size between Gly and Abz micelles was the largest one (12–35), containing 35 hydrophobic repeating units.

Drug Release Study

Drug conjugation through a hydrazone linkage modified with spacers was expected to achieve pH-sensitive release of DOX at either acidic intratumoral or intracellular environment (pH 5.0–6.8). In order to confirm this hypothesis, drug release studies were performed for each of the micelle compositions under sink conditions at physiological pH (7.4) and intracellular pH (5.0) environments (Fig. 5). Release of DOX from micelles was observed over 48 h, taking seven readings during that time (0, 0.5, 1, 3, 6, 24 and 48 h). Unexpectedly, drug release occurred for all Gly and Abz micelles at pH 7.4, with 15% or more drugs released after 48 h. Yet, it was noticeable that irrespective of micelle composition, more drugs were released at pH 5.0 than at pH 7.4.

Gly micelles with composition of 12–5 and 12–15 showed very similar release patterns for both pH 5.0 and pH 7.4. Altering the chain length seems to have had little effect on the release patterns for these compositions. 12–35 Gly micelles showed release profiles different from the other two compositions, releasing the least amount of drug in both pH 5.0 and pH 7.4. 12–5 and 12–15 Abz micelles similarly showed little change in their release profiles, while fewer drugs were released from the 12–35 Abz micelles. The trend between the Gly and Abz micelles appears to be similar. Shorter chain length micelles maintained similar release profiles, while longer chain length micelles had differing release profiles.

Table II Particle Size Distribution

Compound	Composition	Particle size[a] (nm)
PEG-p(Asp-Gly-Hyd-DOX)	12–5	43.98 ± 9.32
	12–15	44.59 ± 11.67
	12–35	39.84 ± 4.89
PEG-p(Asp-Abz-Hyd-DOX)	12–5	10.87 ± 2.30
	12–15	24.45 ± 6.38
	12–35	42.67 ± 5.95

[a] Data were obtained by triplicate measurements and shown as average ± standard deviation.

Total drug release, after 48 h, emphasized the effect of pH on drug release (Fig. 6). 12–5 Gly micelles showed 30% release of DOX at pH 7.4, which was increased 40% at pH 5.0. The 12–15 formulation showed similar results to the 12–5 micelles. Forty-four percent of DOX was released at pH 7.4, and the drug release increased to 57% at 5.0 after 48 h. The 12–35 Gly micelles had the least amount of drugs released. Only 37% of drugs were released at pH 5.0, although that was still higher than 17% of drugs released at pH 7.4. For the Abz micelles, the pH difference had a greater effect on the 12–5 and 12–15 formulation. After 48 h, 60% of DOX was released at pH 5.0, and only 36% released at pH 7.4 for the 12–5 Abz micelles. Similarly, for the 12–15 Abz micelles, 65% of DOX was released at pH 5.0, which was lowered to 30% at pH 7.4. The 12–35 Abz micelles again showed the least release at both pH 7.4 and 5.0, with no more than 30% release in either pH.

In addition to pH-dependent drug release patterns in each micelle, significant differences were observed in the total amount of drug released after 48 h for Gly and Abz micelles at pH 5.0. The 12–5 Gly micelles released 40% of DOX, while similar Abz micelles released 60% of drug. This trend continued for 12–15 micelles with 55% of drug released for Gly micelles and 65% for the Abz micelles. However, 12–35 micelles released similar amounts after 48 h, which were 35% and 32% for Gly and Abz micelles, respectively. It must be noted that Gly and Abz micelles released comparable amounts of drug at pH 7.4. For the 12–5 and 12–15 micelles, around 30–40% of drugs were released from both Gly and Abz micelles. Both Gly and Abz micelles with 12–35 composition released slightly less than 20% of drugs. Intriguingly, the 12–15 compositions differed in that Gly micelles released more drugs than the Abz micelles at pH 7.4, although carbazate linkers with a

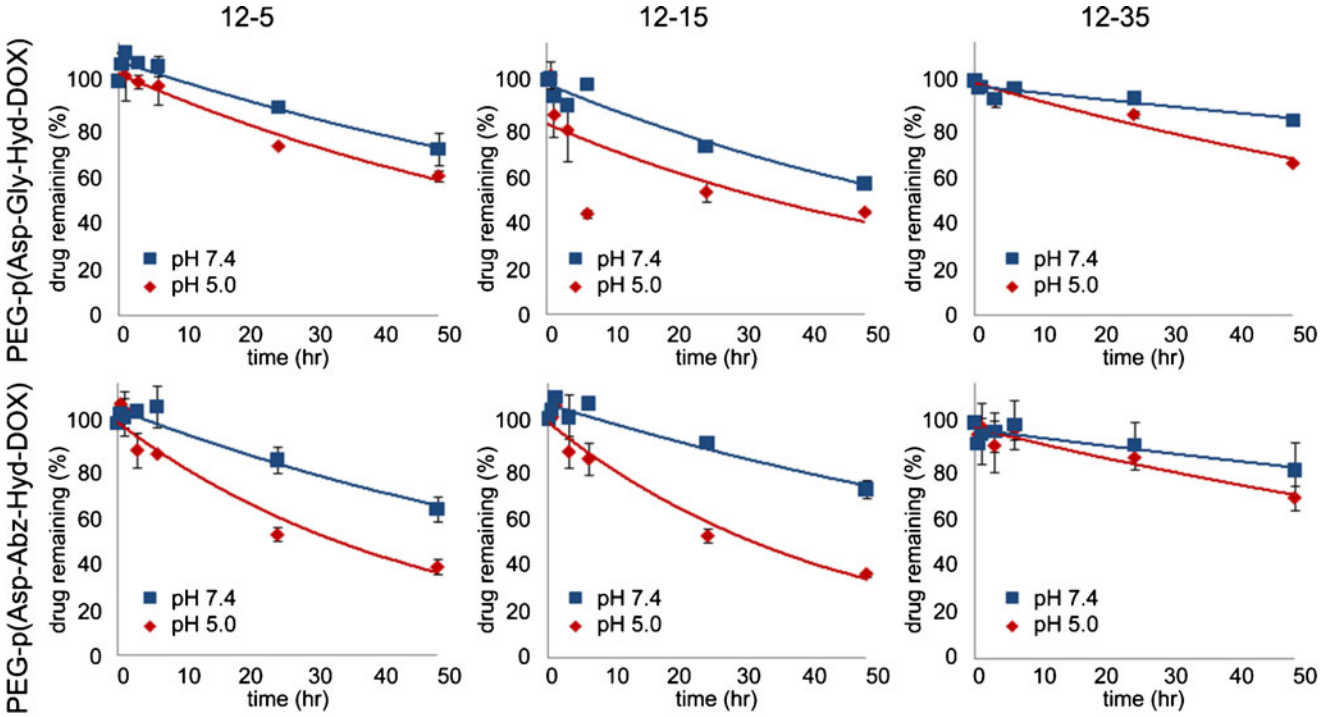

Fig. 5 Drug entrapment stability of polymer micelles at different pH (5.0 and 7.4) for 48 h incubation.

Gly spacer were expected to be more stable than the Abz-modified hydrazone linkage.

At pH 7.4, neither linkers nor chain lengths affected drug release from the micelles with composition of 12–5 and 12–15 (Table III). All four of the micelles had zero-order release constants between 0.7 and 0.9 and first-order constants between 0.008 and 0.012. Increasing the chain length to 35 changed the release kinetics, but rate constants remained comparable for Gly and Abz micelles. Zero-order release constants were 0.2850 for Gly micelles and 0.3351 for Abz micelles, while first-order release rates were 0.003 and 0.004 for Gly and Abz micelles, respectively. The Abz micelles had starkly different profiles than the Gly micelles at pH 5.0, as was further observed through calculated rate constants for zero- and first-order kinetic models. Gly micelles with 12–5 and 12–15 compositions had zero-order release constants close to 1.0 and first-order constants of 0.012 and 0.015, respectively, at pH 5.0. This contrasted Abz micelles, which had zero-order release constants of 1.4 and first-order constants of 0.023 at pH 5.0. This shows a 140% difference between the release constants for either zero- or first-order release in acidic conditions where the micelles are designed to release drugs in a pH-controlled fashion. For the shorter block copolymers, linkers (Gly or Abz) on the side chain seemed to more significantly influence drug release from micelles than chain lengths of block copolymer backbones. To the contrast, the micelles from longer block copolymers (12–35) had comparable drug release rates for both zero- and first-order release, irrespective of linkers.

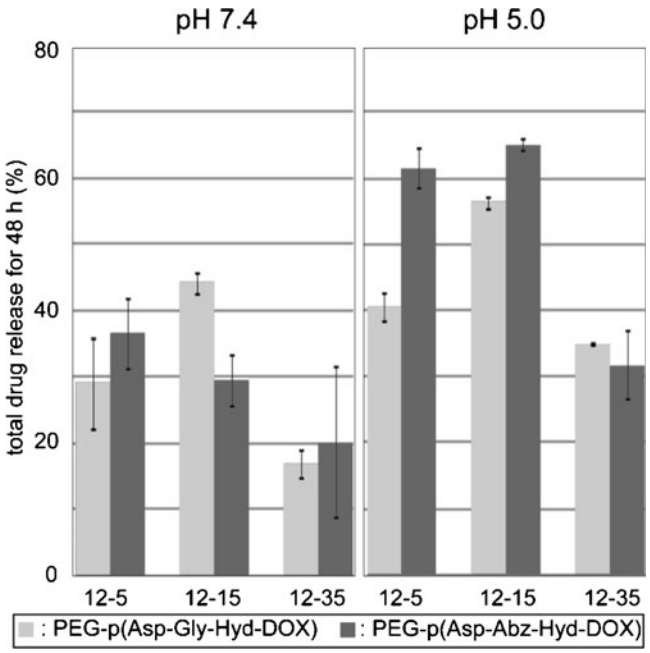

Fig. 6 Quantification of total drug released.

A dramatic contrast was observed when comparing these release rates at pH 5.0 and 7.4 for each micelle composition. For the Gly micelles with 5 and 15 repeating units, there was a 25% increase in both of the zero-order and first-order rate constants. An even greater change was observed for the Abz micelles. A 60% increase was observed for the

Table III Drug Release Analysis*

Compound	pH7.4			pH5.0		
	Composition	k_0	k_1	Composition	k_0	k_1
PEG-p(Asp-Gly-Hyd-DOX)	12–5	0.7713	0.009	12–5	0.9709	0.012
	12–15	0.8346	0.012	12–15	1.0065	0.015
	12–35	0.2850	0.003	12–35	0.6642	0.008
PEG-p(Asp-Abz-Hyd-DOX)	12–5	0.8620	0.010	12–5	1.4311	0.022
	12–15	0.7028	0.008	12–15	1.4342	0.023
	12–35	0.3351	0.004	12–35	0.5901	0.007

*Drug release kinetic parameters were estimated with zero-order (k_0) and first-order (k_1) models.

12–5 micelles, and there was a two-fold increase for the 12–15 compositions. The 12–35 formulation of both Gly and Abz micelles showed similar increase in rate constants, with the release rate constants doubling in each case.

DISCUSSION

In this study, polymer micelles from poly(ethylene glycol)-poly(amino acids) block copolymers, which have been extensively studied for the past decades, are used as a platform to design tunable drug delivery systems (Fig. 1a). DDSs have been developed so far to mainly improve the solubility and tumor-specific accumulation of poorly water-soluble drugs. This approach can be described as spatial control of drug distribution (Fig. 1b). A novel delivery system proposed in this study is expected to achieve temporal control of drug distribution in tumor tissues or other targeted disease lesions (Fig. 1c).

Monomers and Block Copolymer Scaffolds Synthesis

Three compositions of PEG-p(Asp) block copolymers were synthesized for scaffolds to introduce drug-binding linkers with various hydrolysis rates. Synthesis of PEG-p(Asp) was successful and reproducible; controlling the monomer ratio added allows for predictable synthesis. Polymers with 10, 20 and 40 hydrophobic repeating units were initially targeted, and comparable block copolymers were synthesized with p(Asp) repeating units of 5, 15 and 35. There was a slight decrease in actual number of repeating units attributed to partially inactive BLA-NCA. The numbers of repeating units was increased from 5 to 35 in order to observe the effects that the hydrophobic repeating units, after drug-conjugation, had on the micelle stability, drug loading and release rates.

Linker Design and Drug Conjugation

Tunable drug release was achieved by using carbazate drug-binding linkers, which have various hydrolysis rates in a pH-dependent fashion (Fig. 2). Two spacers, Gly and Abz, were inserted into the block-copolymer scaffold using a coupling reaction typically used in solid-phase peptide synthesis (Figs. 3 and 4). After different methods of coupling were attempted due to unsuccessful reactions, using HBTU as the coupling reagent proved to be the key to inserting spacers. It is surmised that the single molecule-mediated coupling mechanism of HBTU seemed to be least influenced by intramolecular steric hindrance at the side chain of PEG-p(Asp) in comparison to other coupling agents, such as DCC, DIC and EDC, with which bulky active esters are involved in the coupling reaction. Solubility of block copolymers, changing as coupling reactions proceeds, could be another factor that made the coupling reaction at the side chain of block copolymers challenging.

Acid-labile hydrazone linkages were employed in this study to control drug release from polymeric micelles. Fig. 4 shows the mechanism of tunable drug release using carbazate drug-binding linkers that lead to hydrazone linkages of drug molecules possessing a ketone group. The benzyl ring of the Abz was expected to increase the release rate (less stable), while the release rate of Gly spacers was expected to be lower (more stable) than that of the Abz. Functional groups adjacent to α-carbonyl of carbazate compounds have been shown to modulate hydrolysis rates of hydrazone linkages with ketone compounds. Electron groups, donating or withdrawing, change the rates of hydrolysis (phenyl > alkyl).

In this study, spacer effects were observed not only on hydrolysis rates but also on apparent drug release patterns accompanied with micelle stability. In addition to the selection of linkers, a model drug was also considered an important factor to properly elucidate the relationship between linker design and drug release patterns. DOX has been shown to be a useful model drug because of its readiness of colorimetric measurements, hydrophobic nature and well-defined functional groups. Moreover, clinically proven therapeutic efficacy of DOX is expected to help elucidate the effects of tunable drug release on tumor chemotherapy in the future in comparison to conventional dosage forms. DOX is an anthracycline antibiotic that has been shown to be effective over a wider range of cancers, but

cytotoxicity has hindered it from reaching its full potential. Drug resistance, both tumors' intrinsic and acquired, has also been associated with DOX. Studies constantly showed that developing a drug delivery system can improve the therapeutic use of DOX.

The degree of drug conjugation differed for each polymer composition (Table I). In respect to weight percent, the drug loading increased as the hydrophobic chain length was extended, due to increasing the number of binding sites. The block copolymers with the smallest chain length provided the least amount of drug bound with one drug molecule per site. Drug loading for the 12–15 compositions was similar, with about 20% drug molecules per binding site, irrespective of the spacer. The largest difference between polymers came from the 12–35 composition, with the drug loading per binding site of PEG-p(Asp-Gly-Hyd-DOX) reaching a high of 44%, while PEG-p(Asp-Abz-Hyd-DOX) only loading 14% of drug with respect to the number binding sites. The extension of the chain length allowed the benzyl ring in PEG-p(Asp-Abz-Hyd-DOX) polymers to cause steric hindrance, making the drug conjugation of DOX less efficient than the PEG-p(Asp-Gly-Hyd-DOX) polymers. Micelles with only 5 hydrophobic repeating units proved to be less promising than those with longer chain length, since only one drug molecule was bound per block copolymer. Micelles with compositions of 12–15 and 12–35 were able to load multiple drugs on the same block copolymer. This allows for high drug loading capacity, maximizing the benefits of micelles. Nevertheless, overall drug conjugation is relatively low in regard to the potential binding sites. Only the PEG-p(Asp-Gly-Hyd-DOX) block copolymer with 35 repeating units showed conjugation greater than 32%. The remaining ones were below that, leaving room for improvement. Coupling of spacers and linkers proved to be challenging. Results suggest that optimizing coupling reactions of spacers as well as drug binding linkers could lead to more effective drug conjugation.

Polymer Micelle Preparation

Polymeric micelles using poly(amino acids) were chosen in this study as the drug carrier due to their flexibility in chemical modifications, imparting functionality without compromising apparent physicochemical properties, such as solubility and particle size. The ketone group of DOX at position 17 allows drug to be easily conjugated to the micelle-forming block copolymer (Fig. 4). Experimental results show that DOX was conjugated to the Hyd of each block copolymer by a hydrazone bond resulting with PEG-p(Asp-Gly-Hyd-DOX) and PEG-p(Asp-Abz-Hyd-DOX). It was previously shown that the hydrazone bond is a facile linkage which is stable at pH 7.4 while cleavable below pH 6 (35). The difference between previous and present studies lies on the linker design, using spacers that can provide different hydrolysis rates. Spacer-modified hydrazone linkers would allow for tunable pH-sensitive drug release in both intratumoral and intracellular regions, while limiting the drug release at physiological pH. Minimizing drug release to regions of the body with a lower pH would reduce the possibility of toxicity. At the same time, greater amounts of drug will be released in the target region, increasing the effectiveness of the chemotherapeutic agent. Polymeric micelles can be defined as self-assembling nano-assemblies in which the inner hydrophobic core contains DOX while the outer hydrophilic provides solubility (38). The micelles are larger in size compared to free DOX and can take advantage of the EPR effect which states that macromolecules accumulate favorably to tumor tissue compared to healthy tissue (39). Such passive accumulation of micelles in tumor sites may decrease the amount of total drug delivered to the body needed for similar therapeutic effect, while lowering cytotoxicity.

The number of hydrophobic repeating units (5, 15, or 35) appeared to increase micelle size, while drug loading yields appeared to decrease their size (Table I and II). The hydrophobic core may tighten with the increase of drug loading, lowering the micelle size (40,41). Abz micelles had similar drug loading per binding size for the three compositions; therefore, the drug loading was held relatively constant. The size of Abz micelles increased from 11 to 43 nm with the lengthening of the hydrophobic segment supporting the hypothesis. To the contrast, Gly micelles had similar micelle size for all three compositions. This may be due to the steady increase of drug loading from 13% to 43.6%, which would increase the hydrophobicity. This would result in a more tightly bound core for polymers with longer chain length, which would decrease the micelle size. For the PEG-p(Asp-Gly-Hyd-DOX), the increase in drug loading decreased the micelle size, while the increase in hydrophobic repeating units simultaneously increased the micelle size. The combination of these two effects seemed to keep Gly micelle size almost constant for all three compositions.

Drug Release Study

The effects of different drug binding linkers and number of different repeating units were observed (Fig. 5). Drug release from the micelles is influenced by both hydrolysis rates of drug binding linkers and diffusion kinetics of drugs from hydrophobic core of micelles; thus, the release profiles of DOX do not simply correspond to the hydrolysis rates of hydrazone linkers. It was still observed that the introduction of functional groups (spacers) next to the carbazate groups of PEG-p(Asp) block copolymers led to differential drug

release patterns, which were also affected by micelle stability. Spacer effects on drug release were significant when polymer micelles were prepared from functional PEG-p(Asp) with shorter chain lengths (12–5 and 12–15). However, drug release patterns were largely influenced by micelle stability, which is presumably due to the increased hydrophobicity of the micelle core-containing spacers with different lipophilicity (aliphatic Gly and aromatic Abz). This was clearly observed at pH 5.0 through the drug release studies (Fig. 6). Release kinetics in Table III showed the similarity in between the 12–5 and 12–15 Gly micelles, as well as the 12–5 and 12–15 Abz micelles. Comparing the 12–5 Gly and Abz micelles, significant differences were observed in the release rates. Abz micelles showed more prominent pH-dependent drug release patterns compared to Gly micelles. This was again shown for 12–15 micelles; the change in the release profiles observed in this paper from the ABZ micelles to the GLY micelles exemplifies that altering the spacers permits drug release to be tuned. It is intriguing that micelle stability became a factor as block copolymer chain lengths increased. Release kinetics of 12–35 micelles were similar irrespective of spacers. Observing total drug release at pH 5.0 after 48 h confirms this trend as well. Shorter chain length polymers showed similar release for Gly and Abz micelles at pH 7.4. Increasing the chain length by 10 repeating units from 5 to 15 seemed to have little effect on drug release patterns, but altering the spacer made a significant change. Micelles with the Abz spacer released fewer drugs at pH 7.4 and more drugs at pH 5.0 than Gly micelles. These results are consistent in that for the longer chain length micelle stability was observed to come into effect since the percent release of the micelles was comparable. Importantly, the side-chain modifications appeared to have almost no effects on micelle integrity or chemical stability of drug-binding linkers. Unexpected drug release occurred at pH 7.4 for all of the micelle compositions, but it was significantly less than release at pH 5.0. It is believed that fine-tuning the block copolymer spacers will allow for drug release to be better controlled.

CONCLUSION

Experimental results demonstrated that PEG-p(Asp) block copolymers with an aliphatic spacer (glycine: Gly) show slower drug release patterns compared to those with an aromatic spacer (aminobenzoate: Abz) when polymer chain lengths were relatively short (12–5 and 12–15). Although short block copolymers have been shown to form unstable micelles or to be incapable of self-assembling, data obtained in this study demonstrate that spacers seem to stabilize micelles retaining sufficient hydrophobicity for self-assembly formation with short block copolymer chains. As micelle-forming block polymers became longer (12–35), drug release from micelles decreased significantly. It is speculated that spacers contributed to formation of overly stable micelles, leading to slower drug release. On the other hand, these results clearly indicate that micelle cores seem to more efficiently protect drug-binding linkers from hydrolysis in longer chain lengths. Therefore, it is concluded that shorter block copolymers are useful to design tunable drug release based on linker stability, while longer block copolymers can be used to achieve tunable drug release exploiting micelle stability.

In conclusion, a collection of six block copolymers, possessing drug-binding linkers with different hydrolysis rates, has been successfully prepared in this study. Anticancer drugs were effectively conjugated to these block copolymers, forming <50 nm nanoassemblies polymer micelles. Prepared polymer micelles showed pH-sensitive drug release patterns in a tunable manner, based on stability of drug-binding linkers as well as micelle structures. PEG-poly(amino acid) block copolymer micelles would provide a promising approach to design a drug delivery system capable of tunable pH-dependent drug release. This will potentially enable the planning of tumor-specific regimens for both early-prompt and late-prolonged chemotherapeutic treatment simultaneously, without compromising pharmacokinetic profiles of drug carriers.

ACKNOWLEDGEMENTS

Authors acknowledge financial support provided by the Kentucky Lung Cancer Research Program.

REFERENCES

1. Scripture CD, Figg WD. Drug interactions in cancer therapy. Nat Rev, Cancer. 2006;6:546–58.
2. Atkins JH, Gershell LJ. Selective anticancer drugs. Nat Rev, Cancer. 2002;1:645–6.
3. Hanahan D, Weinberg RA. The hallmarks of cancer. Cell. 2000;100:57–70.
4. Duncan R. Polymer conjugates as anticancer nanomedicines. Nat Rev, Cancer. 2006;6:688–701.
5. Senter PD, Kopecek J. Drug carriers in medicine and biology. Mol Pharmacol. 2004;1:395–8.
6. Jain RK RK, Munn LL, Fukumura D. Dissecting tumour pathophysiology using intravital microscopy. Nat Rev, Cancer. 2002;2:266–76.
7. Yamaoka T, Tabata Y, Ikada Y. Distribution and tissue uptake of poly(ethylene glycol) with different molecular weights after intravenous administration to mice. J Pharm Sci. 1994;83:601–6.
8. Maeda H, Matsumura Y. Tumoritropic and lymphotropic principles of macromolecular drugs. Crit Rev Ther Drug Carrier Syst. 1989;6:193–210.
9. Kwon G, Kataoka K. Block copolymer micelles as long-circulating drug vehicles. Adv Drug Deliv Rev. 1995;16:295–309.

10. Putnam D, Kopecek J. Polymer conjugates with anticancer activity. Adv Polym Sci. 1995;122:55–123.
11. Duncan R. The dawning era of polymer therapeutics. Nature Rev Drug Discov. 2003;2:347–60.
12. Tsukioka Y, Matsumura Y, Hamaguchi T, Koike H, Moriyasu F, Kakizoe T. Pharmaceutical and biomedical differences between micellar doxorubicin (NK911) and liposomal doxorubicin (Doxil). Jpn J Cancer Res. 2002;93:1145–53.
13. Matsumura Y, Maeda H. A new concept for macromolecular therapeutics in cancer chemotherapy: mechanism of tumoritropic accumulation of proteins and the antitumor agent SMANCS. Cancer Res. 1986;46:6387–92.
14. Stella B, Arpicco S, Peracchia MT, Desmaele D, Hoebeke J, Renoir M *et al.* Design of folic acid-conjugated nanoparticles for drug targeting. J Pharm Sci. 2000;89:1452–64.
15. Takakura Y, Hashida M. Macromolecular carrier systems for targeted drug delivery: pharmacokinetic considerations on biodistribution. Pharm Res. 1996;13:820–31.
16. Benelli R, Monteghirfo S, Balbi C, Barboro P, Ferrari N. Novel antivascular efficacy of metronomic docetaxel therapy in prostate cancer: hnRNP K as a player. Int J Cancer. 2009;124:2989–96.
17. Mayer LD, Harasym TO, Tardi PG, Harasym NL, Shew CR, Johnstone SA *et al.* Ratiometric dosing of anticancer drug combinations: controlling drug ratios after systemic administration regulates therapeutic activity in tumor-bearing mice. Mol Cancer Ther. 2006;5:1854–63.
18. Patel M, Ardalan K, Hochman I, Tian EM, Ardalan B. Cytotoxic effects and mechanisms of an alteration in the dose and duration of 5-fluorouracil. Anticancer Res. 2003;23:447–52.
19. Ma J, Waxman DJ. Modulation of the antitumor activity of metronomic cyclophosphamide by the angiogenesis inhibitor axitinib. Mol Cancer Ther. 2008;7:79–89.
20. Bae Y, Kataoka K. Intelligent polymeric micelles from functional poly(ethylene glycol)-poly(amino acid) block copolymers. Adv Drug Deliv Rev. 2009;61:768–84.
21. Lavasanifar A, Samuel J, Kwon G. Poly(ethylene oxide)-block-poly(L-amino acid) micelles for drug delivery. Adv Drug Deliv Rev. 2002;54:169–90.
22. Kataoka K, Yokoyama M, Kwon GS, Okano T, Sakurai Y. Block copolymer micelles as vehicles for drug delivery. J Control Release. 1993;24:119–32.
23. Blanco E, Kessinger CW, Sumer BD, Gao J. Multifunctional micellar nanomedicine for cancer therapy. Exp Biol Med. 2009;234:123–31.
24. Bae Y, Jang W-D, Nishiyama N, Fukushima S, Kataoka K. Multifunctional polymeric micelles with folate-mediated cancer cell targeting and pH-triggered drug releasing properties for active intracellular drug delivery. Mol BioSyst. 2005;1:242–50.
25. Bae Y, Nishiyama N, Kataoka K. *In vivo* antitumor activity of the folate-conjugated pH-sensitive polymeric micelle selectively releasing adriamycin in the intracellular acidic compartments. Bioconjug Chem. 2007;18:1131–9.
26. Bae Y, Nishiyama N, Fukushima S, Koyama H, Matsumura Y, Kataoka K. Preparation and biological characterization of polymeric micelle drug carriers with intracellular pH-triggered drug release property: tumor permeability, controlled subcellular drug distribution, and enhanced *in vivo* antitumor efficacy. Bioconjug Chem. 2005;16:122–30.
27. Nakanishi T, Fukushima S, Okamoto K, Suzuki M, Matsumura Y, Yokoyama M *et al.* Development of the polymer micelle carrier system for doxorubicin. J Control Release. 2001;74:295–302.
28. Suzuki H, Nakai D, Seita T, Sugiyama Y. Design of a drug delivery system for targeting based on pharmacokinetic consideration. Adv Drug Deliv Rev. 1996;19:335–57.
29. Kaneko T, Willner D, Monkovic I, Knipe JO, Braslawsky GR, Greenfield RS *et al.* New hydrazone derivatives of adriamycin and their immunoconjugates—a correlation between acid stability and cytotoxicity. Bioconjug Chem. 1991;2:133–41.
30. West KR, Otto S. Reversible covalent chemistry in drug delivery. Curr Drug Discov Technol. 2005;2:123–60.
31. Kratz F, Beyer U, Schutte MT. Drug-polymer conjugates containing acid-cleavable bonds. Crit Rev Ther Drug. 1999;16:245–88.
32. Lee ES, Gao Z, Bae YH. Recent progress in tumor pH targeting nanotechnology. J Control Release. 2008;132:164–70.
33. Callahan J, Kopeckova P, Kopecek J. Intracellular trafficking and subcellular distribution of a large array of HPMA copolymers. Biomacromolecules. 2009;10:1704–14.
34. Jones AT, Gumbleton M, Duncan R. Understanding endocytic pathways and intracellular trafficking: a prerequisite for effective design of advanced drug delivery systems. Adv Drug Deliv Rev. 2003;55:1353–7.
35. Bae Y, Fukushima S, Harada A, Kataoka K. Design of environment-sensitive supramolecular assemblies for intracellular drug delivery: polymeric micelles that are responsive to intracellular pH change. Angew Chem Int Ed. 2003;42:4640–3.
36. Cammas S, Kataoka K. Functional poly (ethylene oxide)-co-(β-benzyl-L-aspartate) polymeric micelles: block copolymer synthesis and micelles formation. Macromol Chem Phys. 1995;196:1899–905.
37. Yokoyama M, Miyauchi M, Yamada N, Okano T, Kataoka K, Inoue S. Polymer micelles as novel drug carriers: adriamycin-conjugated poly(ethylene glycol)-poly(aspartic acid) block copolymer. J Control Release. 1990;11:269–78.
38. Allen C, Maysinger D, Eisenberg A. Nano-engineering block copolymer aggregates for drug delivery. Colloids Surf, B Biointerfaces. 1999;16:3–27.
39. Kataoka K, Matsumoto T, Yokoyama M, Okano T, Sakurai Y, Fukushima S *et al.* Doxorubicin-loaded poly(ethylene glycol)-poly (β-benzyl-L-aspartate) copolymer micelles: their pharmaceutical characteristics and biological significance. J Control Release. 2000;64:143–53.
40. Fukushima S, Machida M, Akutsu T, Shimizu K, Tanaka S, Okamoto K *et al.* Roles of adriamycin and adriamycin dimer in antitumor activity of the polymeric micelle carrier system. Colloids Surf, B Biointerfaces. 1999;16:227–36.
41. Yokoyama M, Satoh A, Sakurai Y, Okano T, Matsumura Y, Kakizoe T *et al.* Incorporation of water-insoluble anticancer drug into polymeric micelles and control of their particle size. J Control Release. 1998;55:219–29.